Synthesis and Hierarchical Superstructures of Side-Chain Liquid Crystal Polyacetylenes Containing Galactopyranoside End-Groups

MING-SHOU HO, CHAIN-SHU HSU

Department of Applied Chemistry, National Chiao Tung University, Hsinchu, Taiwan 30010, Republic of China

Received 23 July 2009; accepted 24 August 2009
DOI: 10.1002/pola.23702
Published online in Wiley InterScience (www.interscience.wiley.com).

ABSTRACT: Three kinds of chiral saccharide-containing liquid crystalline (LC) acetylenic monomers were prepared by click reaction between 2-azidoethyl-2,3,4,6-tetraacetyl-β-D-galactopyranoside and 1-biphenylacetylene 4-alkynyloxybenzoate. The obtained monomers were polymerized by WCl_6-Ph_4Sn to form three side-chain LC polyacetylenes containing 1-[2-(2,3,4,6-tetraacetyl-β-D-galactopyranos-1-yl)-ethyl]-1*H*-[1,2,3]-triazol-4′-biphenyl 4-alkynyloxybenzoate side groups. All monomers and polymers show a chiral smectic A phase. Self-assembled hiearchical superstructures of the chiral saccharide-containing LCs and LCPs in solution state were studied by field-emission scanning electron microscopy. Because of the LC behavior, the LC molecules exhibit a high segregation strength for phase separation in dilute solution (THF/H_2O = 1:9 v/v). The self-assembled morphology of LC monomers was dependent upon the alkynyloxy chain length. Increasing the alkynyloxy chain length caused the self-assembled morphology to change from a platelet-like texture (**LC-6**) to helical twists morphology (**LC-11** and **LC-12**). Furthermore, the helical twist morphological structure can be aligned on the polyimide rubbed glass substrate to form two-dimensional ordered helical patterns. In contrast to LC monomers, the **LCP-11** self-assembled into much more complicate morphologies, including nanospheres and helical nanofibers. These nanofibers are evolved from the helical cables ornamented with entwining nanofibers upon natural evaporation of the solution in a mixture with a THF/methanol ratio of 3:7. © 2009 Wiley Periodicals, Inc. J Polym Sci Part A: Polym Chem 47: 6596–6611, 2009

Keywords: liquid-crystalline polymers (LCP); polyacetylenes; self-assembly

INTRODUCTION

Liquid crystalline (LC) materials have large anisotropy of optical, electrical, magnetic, and physical properties because of their anisotropy molecular structure and molecular alignment. They can show a variety of characteristic behavior on application of electric and magnetic fields.[1] On the other hand, conjugated polymers with highly extended π-conjugation in their main chain have many potential applications such as sensors,[2] light-emitting diodes,[3] and photovoltaic devices.[4] Recently, a variety of LC conjugated polymers having a mesogenic part in their side-chains were synthesized and characterized. Such kinds of new conjugated polymers, which can be aligned under LC phase, are useful for the application in organic

Correspondence to: C.-S. Hsu (E-mail: cshsu@mail.nctu.edu.tw)

Journal of Polymer Science: Part A: Polymer Chemistry, Vol. 47, 6596–6611 (2009)

electronics.[5] In particular, much attention has been paid to LC polyacetylenes, which have been widely studied by several research groups.[6–14]

Helical polymers such as naturally occurring proteins and genes have precisely ordered hierarchical architectures and have broad potential applications including molecular recognition (chiral separation, sensory functions) and LC formation through well-ordered molecular alignment.[15–17] The helix can be found among the most sophisticated and fundamental structures of the polymer chain because its characteristic features can be expected for synthetic helical polymers. Therefore, based on the optically active helical structure, synthetic helical polymers have been investigated during the past decade because of their unique properties.[18]

Among the synthetic helical polymers, polyacetylenes have been extensively studied. Moore et al.[19] reported that polyacetylenes with a chiral substituent have predominantly a single sense of helix due to the nonplanar conformation of the polyene structure. For the polyacetylene-based helical polymers, previous studies have mostly focused on poly(phenylacetylenes) with chiral substituents. This is because high stereoregularity is indispensable for the construction of well-ordered helical polymers.[20] Tang and coworkers[21] synthesized several series of amphiphilic poly(phenylacetylenes) carrying amino acid pendants which were self-assembled into micellar spheres, helical cables, and nanofibers in solution. Yashima et al. reported several unique chirality-responsive helical polymers, such as poly(phenylacetylenes) bearing functional pendant groups as an excess of a single-handed helix through noncovalent bonding interaction, which provides an efficient chirality-sensing system.

In this study, we will focus on the synthesis and self-assembled superstructures of poly(alkylacetylenes). Three LC polymers were prepared by polymerization of acetylenic monomers using transition metals, such as WCl_6-Ph_4Sn as an initiator. The polymers comprise of conjugated polyacetylene backbones, 4-biphenylbenzoate mesogen, and galactopyranoside end group. Self-assembled superstructures of the obtained saccharide-containing LCs and LCPs in solution were studied. To our knowledge, this is the first example of a LC polyacetylene containing a saccharide chiral entity used to explore its self-assembly behavior.

In addition, we aim to study orientation control of helical morphology formed by the chiral LC molecules. The fabrication of two-dimensional (2D) ordered alignment of chiral molecules on substrates is the great challenges in materials science.[22] The supramolecular self-assembly concept has been intensively applied to create 2D chiral surfaces through epitaxial adsorptions and alignments of chiral molecules on metals and highly oriented pyrolytic graphite (HOPG).[23] Here, we utilized rubbed polyimide (PI) alignment layers to control the orientation of the self-assembled helices. This method has been widely used in the production of liquid-crystal displays in which LC molecules can be aligned homogeneously by the rubbed PI layers. In the similar manner, we expect the self-assembled morphology to be aligned epitaxially on the PI alignment layers to form 2D ordered superstructures.[24]

EXPERIMENTAL

Materials

1-(3-Dimethylaminopropyl)-3-ethylcarbodiimide hydrochloride (EDCI), 4-Dimethylaminopyridine (DMAP) (from Aldrich), tungstun(VI) chloride, tetraphenyltin (from Strem) were used as received. The solvents were dried according to standard procedures. Tetrahydrofuran (THF) was distilled under a nitrogen atmosphere over sodium benzophenone ketyl just before use. Dichloromethane (DCM) and toluene were dried over calcium hydride and then distilled under nitrogen. Triethylamine (Et_3N) was distilled and dried over potassium hydroxide.

Characterization Techniques

^1H and ^{13}C NMR spectra (300 MHz) were recorded on a Varian VXR-300 spectrometer. Mass spectra were obtained using a JEOL JMS-HX 110 mass spectrometer. Thermal transitions and thermodynamic parameters were determined by using a Seiko EXSTAR 6000 differential scanning calorimeter (DSC) equipped with a liquid nitrogen cooling accessory. DSC unit operated at heating and cooling rates of 10 °C/min. A 5–10 mg sample of purified material was placed on an aluminum pan and measured against another empty pan as a reference. Thermogravimetric analysis (TGA) was undertaken using a Perkin-Elmer Pyris 1 instrument. The thermal decomposition temperature (T_d) was read at a temperature at which 5% weight loss occurred while heating at a rate of 10 °C/min under a nitrogen atmosphere. A Carl-Zeiss Axiphot optical polarized microscope

equipped with a Mettler FP82 hot stage and a FP80 central processor was used to observe the thermal transitions and to analyze the anisotropic textures. Gel permeation chromatography (GPC) assembled from a Viscotek T50A differential viscometer and a LR125 laser refractometer were used to measure the molecular weights of polymers relative to polystyrene standards. The oven temperature was set at 35 °C, and THF was used as eluent with flow rate of 1 mL/min.

UV–vis absorption spectra were recorded on a Hitachi U-3300 spectrophotometer. Circular dichroism (CD) measurements were conducted on a JASCO J-720 spectrophotometer. UV–vis and CD spectroscopy measurements were performed to investigate the specific absorption bands and chiral expressions of the samples in solution. The CD curve has a convex shape in the vicinity of the maximum of a UV–vis absorption band. This kind of characteristic-shape phenomenon is known as the Cotton effect. This effect, which provides structural information, is characterized by the position, magnitude, sign, and shape of the curve. The spectroscopic experiments were carried out in THF solution (1×10^{-4} M) in quartz tubes.

Self-assembly process of LC monomers and LCP polymers is undergone in solution. The chiral saccharide-containing acetylenic LC monomers were aggregated in dilute solution by using 1 mg of compound dissolved in 1 mL of THF, and then introducing 9 mL of deionized water into the well-dissolved solution. For the LC polymers, the solvent mixture was performed in the THF/methanol solution with a ratio of 3:7 (v/v). After sufficient time for aggregation, a drop of the mixture was transferred to a glass substrate. The cast samples were then examined by field-emission scanning electron microscopy (FESEM). FESEM was performed on a JEOL JSM-7100F using accelerating voltages of 0.3 keV. The samples were mounted to brass shims using carbon adhesive and then sputter-coated with 2–3 nm of Pt (the Pt coating thickness was estimated from the calculated deposition rate and experimental deposition time).

Synthesis of Monomers

The synthesis of chiral galactopyranoside-containing acetylenic monomers is outlined in Scheme 1. 2-Azidoethanol (**1**) and 2-azidoethyl-2,3,4,6-tetraacetyl-β-D-galactopyranoside (**2**) were prepared according to previous literature[25,26] procedures and fully characterized.

4′-(2-(Trimethylsilyl)ethynyl)-biphenyl-4-ol (3)

4′-Bromo-4-hydroxybiphenyl (10.0 g, 40.1 mmol), CuI (0.61 g, 3.2 mmol), bis(tripheny1phosphine)-palladium dichloride [$PdCl_2(PPh_3)_2$] (0.56 g, 0.8 mmol), and PPh_3 (0.84 g, 3.2 mmol) were dissolved in Et_3N (150 mL), and the mixture was stirred under nitrogen. Once all catalysts had been dissolved, (trimethylsilyl) acetylene (6.8 mL, 48.2 mmol) was added. The resulting solution was reacted at 70 °C for 15 h. After Et_3N was removed under reduced pressure, the product was extracted with diethyl ether. The crude product was isolated by evaporating the solvent and purified by column chromatography (silica gel, ethyl acetate/*n*-hexane 1/4 as eluent) to afford white crystals in 95% yield (10.17 g). Purity: 99+% (HPLC). mp 160 °C. $R_f = 0.43$ (silica gel, ethyl acetate/*n*-hexane 1/4).

^{1}H NMR ($CDCl_3$): $\delta = 7.47$ (m, 6H, aromatic protons), 6.89 (d, 2H, $J = 3.30$ Hz, aromatic protons), 4.94 (s, 1H, —OH), 0.24 (s, 9H, —Si(CH_3)$_3$). ^{13}C NMR ($CDCl_3$): $\delta = 155.41$, 141.34, 131.21, 129.92, 128.34, 126.48, 120.29, 115.25, 105.53, 93.01, 0.50. MS (EI, observed m/z): 266. HRMS (m/z) Calcd for $C_{17}H_{18}OSi$: 266.4097, found: 266.4501.

4′-(1-Ethynyl)-biphenyl-4-ol (4)

Tetrabutylammonium fluoride (TBAF) (21 mL, 1 M/THF, 21.0 mmol) was added to a stirred solution of **3** (5.02 g, 18.8 mmol) in THF (5 mL) at ambient temperature. The reaction mixture was stirred for 1 h. Once solvent had been evaporated, the brown residue was partitioned (CH_2Cl_2/$NaHCO_{3(aq)}$). The organic layer was washed (brine), dried ($MgSO_4$), and evaporated. The residue was purified by column chromatography (ethyl acetate/*n*-hexane 1/8) to give 3.17 g of white crystals (87% yield). Purity: 99+% (HPLC). mp 168 °C. $R_f = 0.33$ (silica gel, ethyl acetate/*n*-hexane 1/4).

^{1}H NMR ($CDCl_3$): $\delta = 7.47$ (m, 6H, aromatic protons), 6.89 (d, 2H, $J = 8.40$ Hz, aromatic protons), 4.91 (s, 1H, —OH), 3.09 (s, 1H, —C≡CH). ^{13}C NMR ($CDCl_3$): $\delta = 155.39$, 141.07, 133.00, 132.52, 128.34, 126.48, 120.29, 115.75, 83.63, 77.55. MS (EI, observed m/z): 194. HRMS (m/z) Calcd for $C_{14}H_{10}O_3$: 194.2286, found: 194.2296.

1-[2-(2,3,4,6-Tetraacetyl-β-D-galactopyranos-1-yl)-ethyl]-1H-[1,2,3]-triazol-4′-bi-phenyl-4-ol (5)

Compound **2** (3.24 g, 7.8 mmol), **4** (1.51 g, 7.8 mmol, 1 eq), and CuI (0.74 g, 3.9 mmol) were

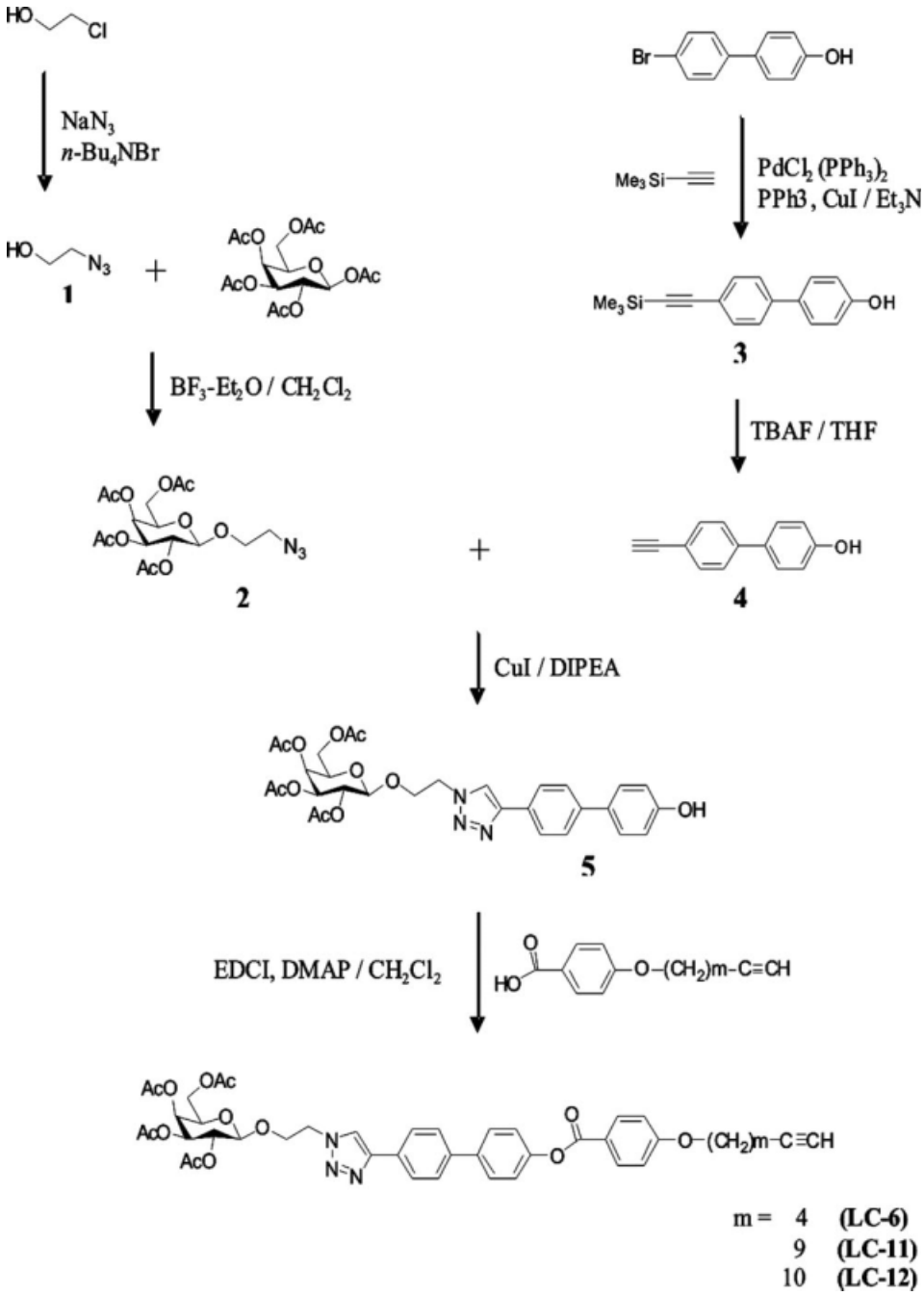

Scheme 1. Synthesis of saccharide-containing acetylenic LC monomers (**LC-6**, **LC-11**, and **LC-12**).

dissolved in dry THF. To this mixture diisopropylethylamine (DIPEA) (1.5 mL, 7.76 mmol) was added and the vial was capped. After stirring for 24 h at room temperature, the mixture was filtered over Celite and the solvent was evaporated under reduced pressure. Further purification was performed using column chromatography (silica gel, ethyl acetate/*n*-hexane 2/1 as eluent) to give 3.1 g of white crystals (65% yield). Purity: 99+% (HPLC). mp 105 °C. $R_f = 0.30$ (silica gel, ethyl acetate/*n*-hexane 2/1). $[\alpha]_D^{29} = -2.16$ (*c* 1, $CHCl_3$).

^{1}H NMR ($CDCl_3$): δ = 7.90 (d, 2H, J = 8.10 Hz), 7.89 (s, 1H), 7.59 (d, 2H, J = 8.10 Hz), 7.49 (d, 2H, J = 8.40 Hz), 6.96 (d, 2H, J = 8.40 Hz), 5.39 (d, 1H, J = 3.30 Hz), 5.23 (m, 1H), 4.98 (dd, 1H, J = 10.50 Hz, J = 3.60 Hz), 4.72 (m, 1H), 4.57

(m, 1H), 4.45 (d, 1H, $J = 7.80$), 4.31 (m, 1H), 4.14 (m, 2H), 3.92 (m, 2H), 2.15 (s, 3H), 2.05 (s, 3H), 1.97 (s, 3H), 1.75 (s, 3H). ^{13}C NMR ($CDCl_3$): $\delta =$ 170.48, 170.23, 170.08, 169.91, 156.01, 147.36, 140.58, 132.54, 128.43, 128.07, 126.90, 126.04, 121.58, 115.85, 100.79, 70.79, 70.52, 68.49, 67.66, 66.83, 61.17, 50.11, 20.64, 20,59, 20.55, 20.50. MS (EI, observed m/z): 611. HRMS (m/z) Calcd for $C_{30}H_{33}N_3O_{11}$: 611.5965, found: 611.5971.

1-[2-(2,3,4,6-Tetraacetyl-β-D-galactopyranos-1-yl)-ethyl]-1H-[1,2,3]-triazol-4′-bi-phenyl 4-alkynyloxybenzoate (LC-6, LC-11, and LC-12)

All three monomers were prepared by esterification of compound **5** with corresponding 4-(alkynyloxy)benzoic acid. An example for the synthesis of **LC-11** is described as follows.

A solution of EDCI (0.3 g, 1.57 mmol) in dichloromethane (30 mL) was added dropwise to a solution of **5** (0.8 g, 1.31 mmol), 4-(undec-10-ynyloxy)benzoic acid (0.41 g, 1.44 mmol) and DMAP (0.02 g, 0.16 mmol) in dichloromethane (10 mL) at 0 °C. After complete addition, the reaction mixture was allowed to stir overnight at room temperature. The reaction progress was monitored by TLC. The resulting mixture was washed twice with an 1 M sodium hydroxide solution and two times with distilled water. The organic layer was dried with anhydrous magnesium sulfate and then evaporated under reduced pressure to give the crude product. Further purification was performed using column chromatography (silica gel, ethyl acetate/*n*-hexane 1/1 as eluent) to give 0.9 g of white crystals (90% yield). Purity: 99+% (HPLC). $R_f = 0.10$ (silica gel, ethyl acetate/*n*-hexane 1/1). $[\alpha]_D^{29} = -3.03$ (c 1, $CHCl_3$).

^{1}H NMR ($CDCl_3$): $\delta = 8.14$ (d, 2H, $J = 8.70$ Hz, aromatic protons), 7.96 (d, 2H, $J = 7.80$ Hz, aromatic protons), 7.90 (s, 1H, —C_2N_3H—), 7.65 (d, 4H, $J = 8.70$ Hz, aromatic protons), 7.27 (d, 2H, $J = 8.70$ Hz, aromatic protons), 6.96 (d, 2H, $J = 9.00$ Hz, aromatic protons), 5.38 (d, 1H, $J = 3.30$ Hz), 5.22 (m, 1H), 4.96 (dd, 1H, $J = 10.50$ Hz, $J = 3.30$ Hz), 4.70 (m, 1H), 4.58 (m, 1H), 4.43 (d, 1H, $J = 7.80$), 4.30 (m, 1H), 4.17 (m, 2H), 4.05 (m, 2H), 3.90 (m, 2H), 2.20–2.15 (m, 5H, —$COOCH_3$ and —$CH_2C{\equiv}CH$), 2.04 (s, 3H, —$COOCH_3$), 1.99–1.91 (m, 4H, —$COOCH_3$ and —$C{\equiv}CH$), 1.84–1.73 (m, 5H, —$COOCH_3$ and —OCH_2CH_2), 1.54–1.32 (m, 12H, —$(CH_2)_6CH_2C{\equiv}CH$). ^{13}C NMR ($CDCl_3$): $\delta =$ 170.35, 170.12, 169.98, 169.72, 164.97, 163.56, 150.64, 147.16, 140.09, 138.12, 132.29, 129.43, 127.95, 127.44, 126.12, 122.16, 121.63, 121.44, 114.29, 100.86, 84.72 (1C, —$C{\equiv}CH$), 70.85, 70.52, 68.47, 68.28, 68.04, 67.57, 66.83, 61.17, 50.12, 29.36, 29.26, 29.06, 28.99, 28.68, 28.43, 25.93, 20.65, 20,62, 20.55, 20.51, 18.37. MS (FAB; observed m/z): 882. HRMS (m/z) Calcd for $C_{48}H_{55}N_3O_{13}$: 881.9626, found: 881.9659.

LC-6. White crystals. Yield 85%. Purity: 99+% (HPLC). $R_f = 0.50$ (silica gel, ethyl acetate/*n*-hexane 2/1). $[\alpha]_D^{29} = -3.13$ (c 1, $CHCl_3$).

^{1}H NMR ($CDCl_3$): $\delta = 8.17$ (d, 2H, $J = 9.00$ Hz, aromatic protons), 7.98 (d, 2H, $J = 8.10$ Hz, aromatic protons), 7.92 (s, 1H, —C_2N_3H—), 7.68 (d, 4H, $J = 8.10$ Hz, aromatic protons), 7.30 (d, 2H, $J = 8.40$ Hz, aromatic protons), 6.99 (d, 2H, $J = 9.00$ Hz, aromatic protons), 5.40 (d, 1H, $J = 3.00$ Hz), 5.24 (m, 1H), 4.98 (dd, 1H, $J = 10.50$ Hz, $J = 3.30$ Hz), 4.70 (m, 1H), 4.58 (m, 1H), 4.46 (d, 1H, $J = 8.10$), 4.31 (m, 1H), 4.16 (m, 2H), 4.09 (m, 2H), 3.92 (m, 2H), 2.31 (td, 2H, $J = 6.90$ Hz, $J = 2.40$ Hz, —$CH_2C{\equiv}CH$), 2.16 (s, 3H, —$COOCH_3$), 2.06 (s, 3H, —$COOCH_3$), 2.00 (t, 1H, $J = 2.70$ Hz, —$C{\equiv}CH$), 1.97–1.93 (m, 5H, —$COOCH_3$ and —OCH_2CH_2), 1.80–1.75 (m, 5H, —$COOCH_3$ and —$CH_2CH_2C{\equiv}CH$). ^{13}C NMR ($CDCl_3$): $\delta =$ 170.34, 170.11, 169.97, 169.69, 164.91, 163.34, 150.55, 147.14, 139.96, 138.10, 132.27, 129.52, 127.91, 127.39, 126.05, 122.21, 121.58, 121.53, 114.23, 100.81, 83.86 (1C, —$C{\equiv}CH$), 70.79, 70.49, 68.78, 68.42, 67.69, 67.55, 66.80, 61.15, 50.02, 28.03, 24.87, 20.64, 20,60, 20.55, 20.49, 18.08. MS (FAB; observed m/z): 812. HRMS (m/z) Calcd for $C_{43}H_{45}N_3O_{13}$: 811.8297, found: 811.8217.

LC-12. White crystals. Yield 90%. Purity: 99+% (HPLC). $R_f = 0.45$ (silica gel, ethyl acetate/*n*-hexane 3/1). $[\alpha]_D^{29} = -3.07$ (c 1, $CHCl_3$).

^{1}H NMR ($CDCl_3$): $\delta = 8.17$ (d, 2H, $J = 8.70$ Hz, aromatic protons), 7.98 (d, 2H, $J = 8.10$ Hz, aromatic protons), 7.92 (s, 1H, —C_2N_3H—), 7.68 (d, 4H, $J = 8.40$ Hz, aromatic protons), 7.30 (d, 2H, $J = 8.40$ Hz, aromatic protons), 6.99 (d, 2H, $J = 9.00$ Hz, aromatic protons), 5.40 (d, 1H, $J = 3.30$ Hz), 5.24 (m, 1H), 4.98 (dd, 1H, $J = 10.50$ Hz, $J = 3.30$ Hz), 4.72 (m, 1H), 4.59 (m, 1H), 4.46 (d, 1H, $J = 8.10$), 4.33 (m, 1H), 4.16 (m, 2H), 4.05 (m, 2H), 3.92 (m, 2H), 2.19–2.13 (m, 5H, —$COOCH_3$ and —$CH_2C{\equiv}CH$), 2.03 (s, 3H, —$COOCH_3$), 1.98–1.91 (m, 4H, —$COOCH_3$ and —$C{\equiv}CH$), 1.84–1.72 (m, 5H, —$COOCH_3$ and —OCH_2CH_2), 1.53–1.30 (m, 14H, —$(CH_2)_7CH_2C{\equiv}CH$). ^{13}C NMR ($CDCl_3$): $\delta =$ 170.33, 170.11, 169.96, 169.69, 164.96, 163.55, 150.62, 147.18, 140.03, 138.11, 132.28, 129.50, 127.93, 127.41, 126.09, 122.15, 121.59, 121.42,

114.28, 100.85, 84.75 (1C, —C≡CH), 70.83, 70.51, 68.46, 68.28, 68.05, 67.68, 66.83, 61.16, 50.07, 29.44, 29.37, 29.29, 29.04, 28.69, 28.55, 28.43, 25.93, 20.63, 20,60, 20.55, 20.49, 18.36. MS (FAB; observed m/z): 896. HRMS (m/z) Calcd for $C_{49}H_{57}N_3O_{13}$: 895.9892, found: 895.9815.

General Polymerization Procedure

The monomers were polymerized using WCl_6 as initiator and Ph_4Sn as coinitiator. All polymerization reactions and manipulations were carried out under nitrogen using either an inert-atmosphere glovebox or Schlenk techniques in a vacuum line system, except for the purification of the polymers, which was done in a fume hood. A typical experimental procedure for the polymerization of monomer **LC-11** is given below as an example.

Monomer **LC-11** (0.6 g, 0.68 mmol) was added into a Schlenk tube with a three-way stopcock on the sidearm. The tube was evacuated under vacuum and then flushed with dried N_2 three times through sidearm. Dried THF (8.5 mL) was injected into the tube through a septum to dissolve the monomer. The initiator solution was prepared in another tube by dissolving WCl_6 (55.52 mg, 0.14 mmol) and Ph_4Sn (59.79 mg, 0.14 mmol) in 1.5 mL of toluene. Both tubes were aged at room temperature for 30 min. The monomer solution was then transferred to the initiator solution using a hypodermic syringe. The reaction mixture was stirred at 60 °C under N_2 for 24 h. The solution was then cooled to room temperature, diluted with 2 mL of THF and added dropwise to 300 mL of diethyl ether through a cotton filter with stirring. The polymer was separated by filtration, purified by several reprecipitations from THF solution into diethyl ether, and then dried in a vacuum oven to yield 0.4 g (67% yield) of the final product **LCP-11**.

^{1}H NMR ($CDCl_3$): δ = 8.18 (d, 2nH), 7.96 (d, 2nH), 7.92 (s, nH), 7.64 (d, 4nH), 7.27 (d, 2nH), 6.98 (d, 2nH), 6.81 (s, nH),5.40 (m, nH), 5.22 (m, nH), 4.94 (m, nH), 4.70 (m, nH), 4.58 (m, nH), 4.43 (m, nH), 4.32 (m, nH), 4.17 (m, 2nH), 4.03 (m, 2nH), 3.90 (m, 2nH), 2.23 (m, 2nH), 2.10–2.02 (m, 6nH), 1.99–1.91 (s, 3nH), 1.85–1.62 (m, 5nH), 1.54–1.22 (m, 12nH). GPC: M_n = 251,000, M_w = 410,500, PDI = 1.64. T_g = 97.1 °C. T_d = 265.3 °C.

LCP-6

Yield 65%. ^{1}H NMR ($CDCl_3$): δ = 8.18 (d, 2nH), 7.97 (d, 2nH), 7.90 (s, nH), 7.65 (d, 4nH), 7.32 (d, 2nH), 6.95 (d, 2nH), 6.82 (s, nH), 5.44 (d, nH), 5.22 (m, nH), 4.91 (m, nH), 4.73 (m, nH), 4.56 (m, nH), 4.44 (m, nH, J = 8.10), 4.32 (m, nH), 4.17 (m, 2nH), 4.10 (m, 2nH), 3.94 (m, 2nH), 2.31–2.21 (m, 2nH), 2.16 (s, 3nH), 2.06 (s, 3nH), 1.95–1.90 (m, 5nH), 1.85-1.63 (m, 5nH). GPC: M_n = 99,300, M_w = 118,200, PDI = 1.19. T_g = 57.6 °C. T_d = 277.9 °C.

LCP-12

Yield 60%. ^{1}H NMR ($CDCl_3$): δ = 8.19 (d, 2nH), 7.98 (d, 2nH), 7.93 (s, nH), 7.63 (d, 4nH), 7.30 (d, 2nH), 6.99 (d, 2nH), 6.81 (s, nH), 5.42 (m, nH), 5.21 (m, nH), 4.93 (m, nH), 4.72 (m, nH), 4.59 (m, nH), 4.46 (m, nH), 4.33 (m, nH), 4.16 (m, 2nH), 4.08 (m, 2nH), 3.92 (m, 2nH), 2.22 (m, 2nH), 2.18-2.01 (m, 6nH), 1.98-1.91 (s, 3nH), 1.87–1.65 (m, 5nH), 1.56–1.22 (m, 14nH). GPC: M_n = 73,400, M_w = 148,300, PDI = 2.02. T_g = 65.5 °C. T_d = 270.3 °C.

Bulk Orientation Control

To control the bulk orientation of the helical morphology formed by **LC-11**, a cotton rubbed PI film on the glass was prepared. A drop of the aggregated **LC-11** was then transferred to the rubbed PI coated glass and then the glass slide was put in a vessel for slow solvent evaporation.

RESULTS AND DISCUSSION

Synthesis of Monomers

Scheme 1 outlines the synthetic steps to prepare the saccharide-containing LC acetylenic derivatives. A saccharide entity was prepared using β-D-galactopyranoside with the acetyl protecting group, since the hydroxyl groups (i.e., acidic protons) in D-galactose are poisoning to the transition-metal catalysts used during the polymerizations of acetylenes.[27] 2-Azidoethyl-2,3,4,6-tetraacetyl-β-D-galactopyranoside (**2**) was synthesized by glycosylation of β-D-galactose pentaacetate with 2-azidoethanol. The coupling of (trimethylsilyl)acetylene to biphenyl halide with a palladium catalyst followed by desilylation of the trimethylsilyl protecting group appeared to be a convenient method to prepare hydroxybiphenylacetylene (**4**) in good yields. The immediate compound **5** was prepared by copper(I)-catalyzed regiospecific 1,3-cycloaddition between **2** and **4**. Finally, the esterification of compound **5** with 4-alkynyloxybenzoic acid yielded the LC monomers with different

Table 1. Polymerization of Saccharide-Containing LC Monomers[a]

	Initiator	Solvent	Yield (%)	M_w[b]	M_w/M_n[b]
LCP-6	WCl_6/Ph_4Sn	Toluene	0		
LCP-6	WCl_6/Bu_4Sn	THF/Toluene	0		
LCP-6	WCl_6/Ph_4Sn	THF/Toluene	65	118,200	1.19
LCP-11	WCl_6/Ph_4Sn	THF/Toluene	67	410,500	1.64
LCP-12	WCl_6/Ph_4Sn	THF/Toluene	60	148,300	2.02

[a] Carried out under nitrogen for 24 h at 60 °C; $[M]_0 = 0.2$ M, [Int.] = [coInt.] = 0.2 mM.
[b] Determined by GPC in THF relative to a polystyrene calibration.

alkynyloxy chain lengths. All the monomers were fully characterized by standard spectroscopic methods, from which satisfactory analysis data corresponding to their expected molecular structures were obtained.

Polymerization Reaction

W- and Rh-based compounds are the most widely used initiators for the polymerization of acetylene-based and phenylacetylene-based monomers.[28] Tang et al. found that $[Rh(nbd)\text{-}Cl]_2$ can initiate polymerization of phenylacetylene-based monomers with ester functionalities, but is not an effective initiator for the polymerization of acetylene-based monomers.[29] They also found that WCl_6-Ph_4Sn is the best initiating system for the polymerization of acetylene-based monomers with polar functionalities.[30,31] In this study, all monomers belong to acetylene-based monomers. Therefore, we chose a WCl_6-Ph_4Sn mixture to polymerize the synthesized LC monomer. It is noted that no polymeric product was obtained when using WCl_6-Bu_4Sn to replace WCl_6-Ph_4Sn to initiate the polymerization under the same reaction conditions. The polymerization of the chiral saccharide-containing acetylenic LCs was carried out in anhydrous toluene and THF. In toluene, polymerization proceeded with a brown oligomer precipitated, whereas the reaction system was homogeneous solution throughout the polymerization when a mixed solvent of THF and toluene was used. The present results indicate that toluene is not a good solvent, especially for the polymerization of alkylacetylene containing hydrophilic saccharide end groups. The results of the polymerization with WCl_6-Ph_4Sn catalyst are summarized in Table 1.

Structure Characterization of Polymers

The polymers are characterized by spectroscopic techniques, and all of them give satisfactory analysis data corresponding to their molecular structures. Analyses by ^{13}C NMR spectroscopy confirm that the resonance peaks of acetylenic triple bonds of the monomers have been converted to the olefinic double bonds of the polymers. As shown in Figure 1 as an example, the acetylene carbon atoms of **LC-12** resonate at δ 84.7 ppm; the peak is completely absent in the spectrum of **LCP-12**. This proves that the polymerization is realized via the transformation of triple bond to double bond. All other peaks in the spectra of the monomer and the polymer can be assigned with confidence.

The stereoregularity of the homopolymers was investigated by ^1H NMR spectroscopy. As for the structure of polyacetylenes, at least four possible conformers exist: cis-transoid, cis-cisoid, trans-transoid, and trans-cisoid. The chemical shift and line shape of the main chain's olefinic protons and aromatic protons are considered to be sensitive to the conformers.[32] According to Percec and coworkers[33] and Tang et al.,[30] the chemical shift of

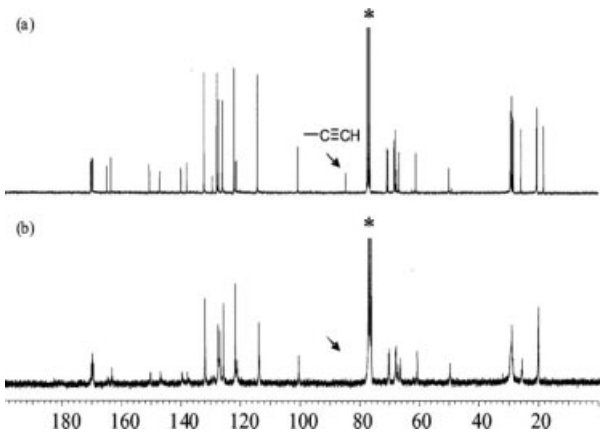

Figure 1. ^{13}C NMR spectra of (a) monomer **LC-12** and (b) its polymer **LCP-12** in chloroform-d. The resonance peaks of the acetylene carbon atoms are marked with solid arrows, while the solvents peak are labeled with asterisks (*).

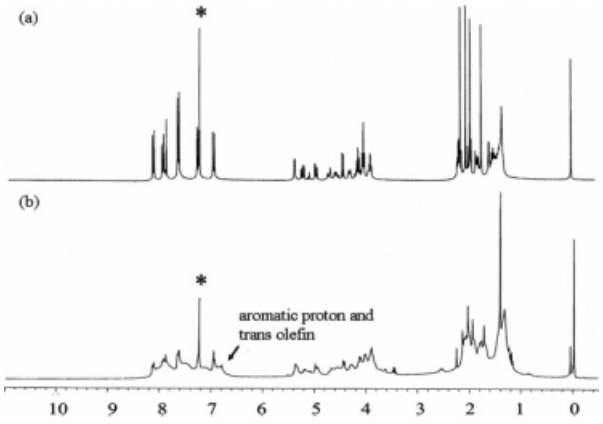

Figure 2. ^{1}H NMR spectra of (a) monomer **LC-12** and (b) its polymer **LCP-12** in chloroform-d. The solvents peaks are marked with asterisks (*).

cis-olefin proton appears in the region 5.88–6.26 ppm for mesogen-containing poly(1-alkynes). Figure 2 depicts the ^{1}H NMR spectra of monomer **LC-12** and polymer **LCP-12**. In the spectra of **LCP-12**, no peak is observed in this region. Therefore, we conclude that the trans-olefin content of polymer **LCP-12** is 100%. Similar observation is found for polymers **LCP-6** and **LCP-11**.

Liquid Crystallinity

The mesomorphic phase behaviors of monomers and polymers were characterized by both differential scanning calorimetry (DSC) and polarized optical microscopy (POM). Their phase transition temperatures are summarized in Table 2. Based on the polarized optical texture, all three monomers exhibit a characteristic texture of chiral S_A phase (S_A^*). Figure 3 displays the typical fan texture exhibited by the monomers. Since S_A and S_A^* show similar texture, it is difficult to differentiate only by optical microscopic observation. However, the monomer contains a chiral saccharide end group, a S_A^* phase should be built up. Just like our previously studied saccharide-containing LCs,[34] all three monomers exhibit a glassy state. Their glass transition temperatures are ranging from 57.8 to 66.2 °C. **LC-6** which contains the shortest spacer length shows the highest glass transition temperature (66.2 °C) and isotropic temperature (165.9 °C). All the polymers also show S_A^* mesomorphism. POM micrographs show that all polymers exhibit a homogeneous texture of the S_A^* phase (Fig. 4). However, all samples undergo decomposition at a temperature over 250 °C, which agrees with the thermogravimetry measurement. It should be noted that, despite the degradation which occurred both before and simultaneously with the transition, the disordered mesophase re-appeared upon cooling.

Optical Activity

To examine the chiral character of the saccharide-based entity, UV–vis and CD experiments of chiral saccharide-based LC monomers were performed first. Figure 5(a) shows the UV–vis spectra of three monomers with various alkynyloxy chain lengths in THF. A maximum absorption band at 283 nm appears as a result of π–π^* transitions related to their mesogenic unit, biphenyl benzoate and triazole moieties. The absorption of the biphenyl mesogen containing triazole ring was 37 nm blue-shifted from that biphenyl (246 nm),[35] indicating that this kind mesogenic group was polarized. The monomers did not show any absorption peak at longer wavelengths (above ca. 325 nm), which the absorption peak is assignable to the conjugated polyacetylene backbone. The UV–vis spectra of three polyacetylene LC polymers showed absorption peaks originating from their alternating double-bond backbones. The absorption, however, was quite weak [Fig. 5(b)]. The steric crowding cause by the bulky mesogenic pendant groups and the aggregate of saccharide pendants might have forced the polymer chain coiled, nonplanar conformation, leading to a

Table 2. Thermal Properties of LC Monomers and LC Polyacetylenes

	Phase Transitions, °C[a] (Kcal/mol)	
	Heating	T_d[b]
LC-6	G 66.2 S_A^* 165.9 (10.73) I	283.2
LC-11	G 57.8 S_A^* 165.9 (6.90) I	362.9
LC-12	G 59.1 S_A^* 165.9 (8.46) I	373.8
LCP-6	G 57.6 S_A^* > 250 I[c]	277.9
LCP-11	G 97.1 S_A^* > 250 I[c]	265.3
LCP-12	G 65.5 S_A^* > 250 I[c]	270.3

G, glass transition; S_A, smectic A phase; I, isotropic phase.

[a] Data taken from the first cycle at 10 °C/min.

[b] Determined by TGA. T_d = temperature at which weight loss of 5% occurred.

[c] Data obtained from polarizing optical microscopy, since it is affected by degradation.

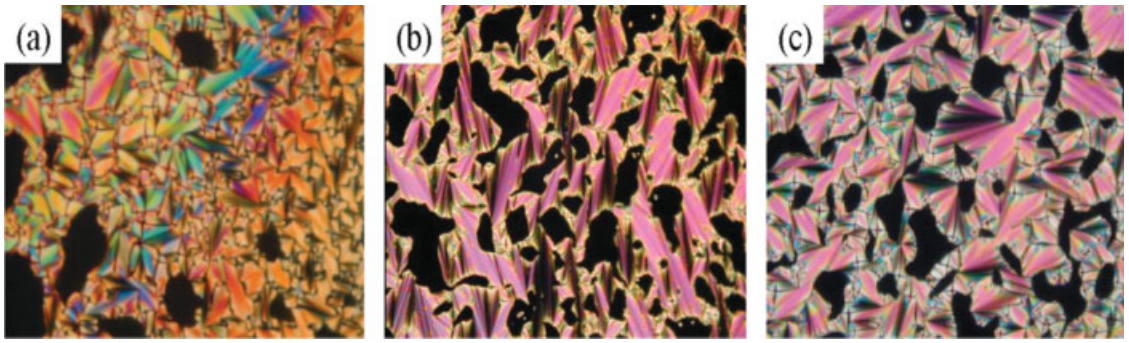

Figure 3. Polarized optical microscopy of the fan-shaped textures exhibited by (a) **LC-6**, (b) **LC-11**, and (c) **LC-12** at 100 °C.

reduction in the effective conjugation length of the polyene backbone (i.e., reducing the intensity of the absorption).[36] In comparison with those of their corresponding monomers, all three polymers show wider UV spectra with a maximum at 280 nm, due to overlap of the π–π^* transitions of the conjugated main chain. Figure 5(c) shows their corresponding CD spectra of the three monomers. As shown from the spectra, three monomers display a typical negative Cotton effect in THF, which comes from β-D-galactopyranoside chiral end group. It means that the bending and twisting forces driven by the chiral saccharide entity can be anticipated in the self-assembly process of three LC monomers.

To characterize the chiroptical properties of polyacetylenes having chiral saccharide pendants, we also used CD spectra to check whether polymer chains have the tendency to induce helical morphology.[37] All chiral polymers in dilute THF solution exhibit intense CD bands with both negative and positive Cotton effects at about 270 and 300 nm [Fig. 5(d)]. In comparison with monomers, negative Cotton effect also comes from β-D-galactopyranoside chiral end group. In addition, all chiral monomers are CD-inactive at wavelengths longer than 290 nm, giving an almost flat line up to the visible spectral region. The positive Cotton effect at ~300 nm thus must be due to the absorption of the polyacetylene backbone, unambiguously confirming that the main chain of the polymer is a helical conformation with a preferred screw sense. Therefore, the main chain of the polymer seems to be chiral, probably due to a predominant one-handed helical sense.

The CD signal reflects both chirality of the main-chain and side-chain aggregation. The interplay between the macromolecular helicity, the chirality of the pendant groups, and the chirality at a macroscopic level are of great interest from fundamental and biological viewpoints. To this end, we have studied the structures of the helical polymers in dilute solution with SEM.

Self-Assembled Hierarchical Superstructures of Saccharide-Containing LC Monomers in Solution

The self-assembled morphology of the chiral saccharide-containing acetylenic LC monomers in solution was examined by FESEM. An interesting

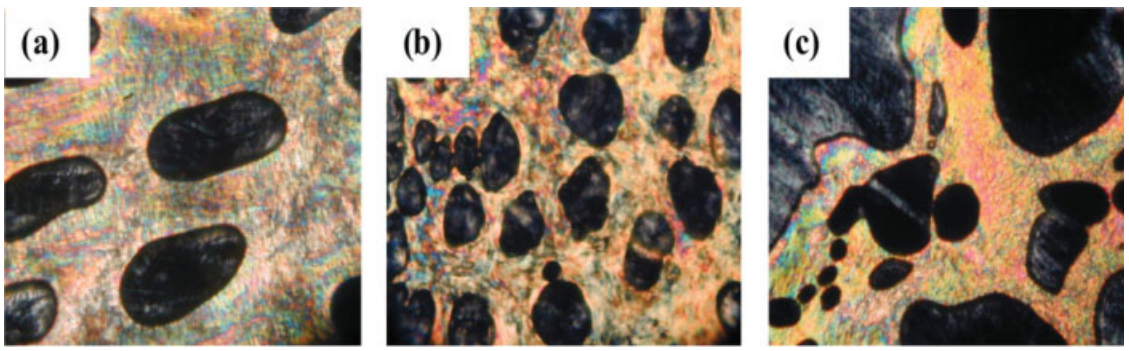

Figure 4. Polarized optical micrographs displayed by (a) **LCP-6**, (b) **LCP-11**, and (c) **LCP-12** at 150 °C.

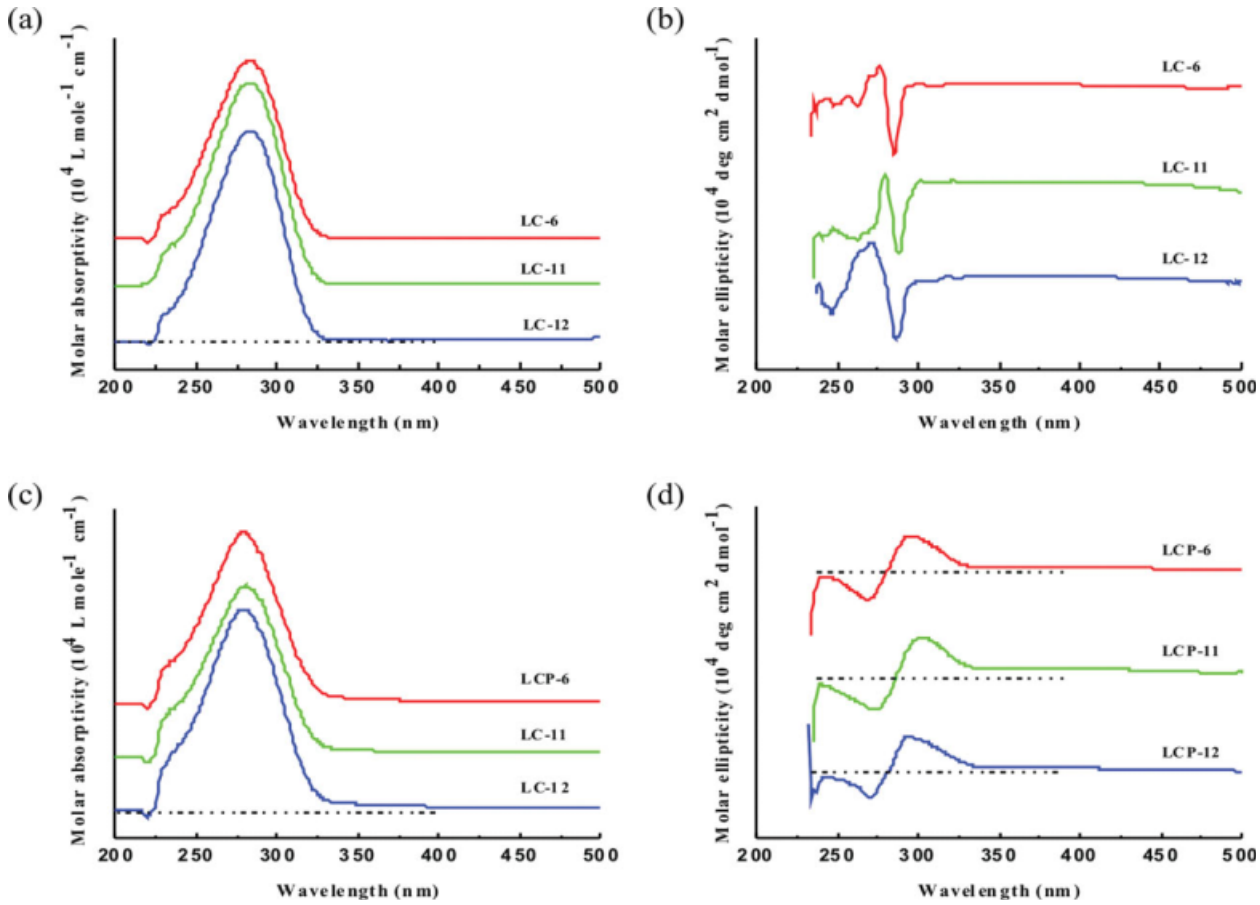

Figure 5. Corresponding UV–vis spectra and CD results of LC monomers (a,b) and LC polymers (c,d) in THF. The spectral data below 250 nm are not taken because of the interfering absorption. [Color figure can be viewed in the online issue, which is available at www.interscience.wiley.com.]

morphological evolution was identified according to the change in the alkynyloxy chain length. **LC-6** exhibits a mixed morphology including a platelet-like morphology and right-handed helical twists, as shown in Figure 6(a). However, the micrographs of **LC-11** and **LC-12** exhibit a right-handed helical morphology in the majority [Fig. 6(b,c)]. The hierarchical aggregates composed of several helical strands were further visualized in the FESEM micrographs. It is also noted that the pitch length of the helical twists decreases with increasing alkynyloxy chain length. These results agree with our previous investigation on the saccharide-containing LC molecules.[34] The helicity of the LC molecules is primarily by the chiral saccharide end group. However, the helicity is amplified in LC state because rod segments π–π interaction leads to liquid-crystalline-like aggregation. This will stabilize the helical morphology.

Orientation Control of the Helical Morphology Exhibited by LC Monomers

We investigated the rubbed induced helical alignment of **LC-11**. Figure 7(b–d) shows the polarized optical micrographs with gypsum plate of the oriented **LC-11** film observed under crossed polarizers. Flat and elongated film is seen. The **LC-11** film is oriented parallel to the rubbing direction, as evidenced by the fact that the counterclockwise [Fig. 7(b)] and clockwise [Fig. 7(d)] images tilted at -45° and $+45^\circ$ with respect to the transmission axis of the polarizer, respectively, showed a clear change of birefringence.

The helical morphology in order 2D arrays is investigated by FESEM. The **LC-11** molecules spontaneously self-assembled into a highly ordered monolayer without helical structure as evidenced by parallel thin plates [Fig. 8(a), red arrow]. This indicates that the molecules lie flat on the surface with a planar conformation,

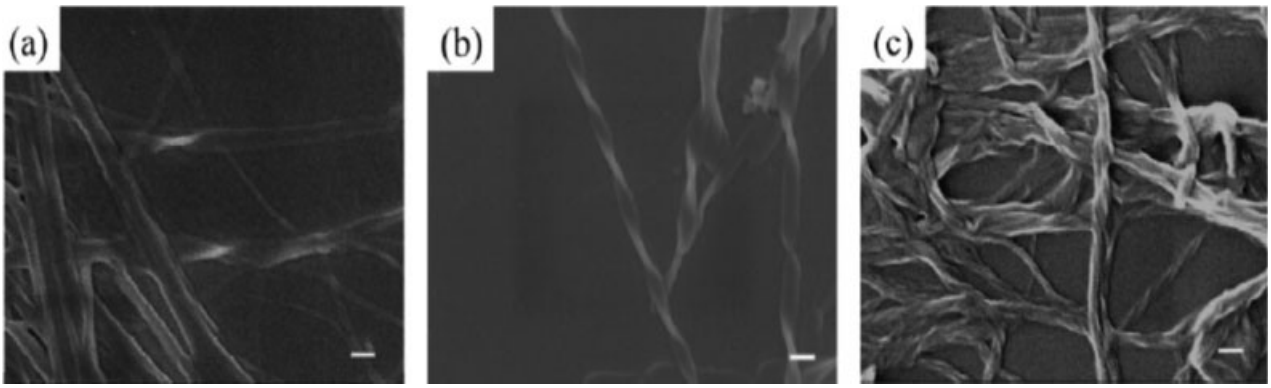

Figure 6. FESEM micrographs of the self-assembled morphology exhibited by monomers (a) **LC-6**, (b) **LC-11**, and (c) **LC-12**. The bar represents 100 nm.

probably because of the strong and epitaxial adsorption of molecules on the surface. The orientation of these plates in the first layer was anticipated to be influenced by that rubbed PI and was nearly parallel to the rubbing direction.

Although the second layer of molecules deposited on this 2D ordered first monolayer appeared to be formless with no specific aggregations [blue arrow in Fig. 8(a)], they further self-assembled into well-defined helix. In the SEM image, 2D

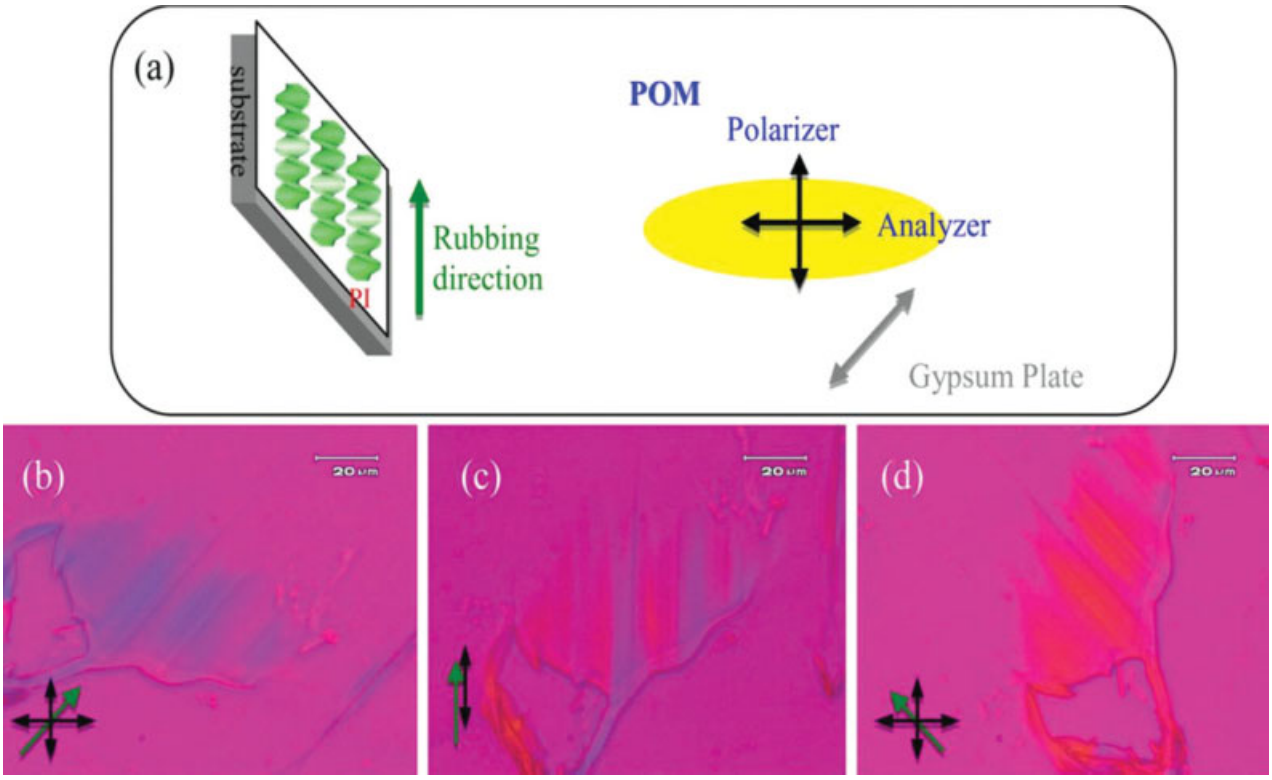

Figure 7. Alignment of helical **LC-11** on rubbed PI substrate. (a) Schematic representation of the rubbed induced alignment of **LC-11** molecules. (b–d) Polarized optical micrographs with gypsum plate of oriented **LC-11** film under crossed polarizers. The substrate was tilted at −45° (b, counterclockwise), 0° (c, parallel), and +45° (d, clockwise) to the transmission axis of the polarizer. The green arrows indicate the rubbing direction. [Color figure can be viewed in the online issue, which is available at www.interscience.wiley.com.]

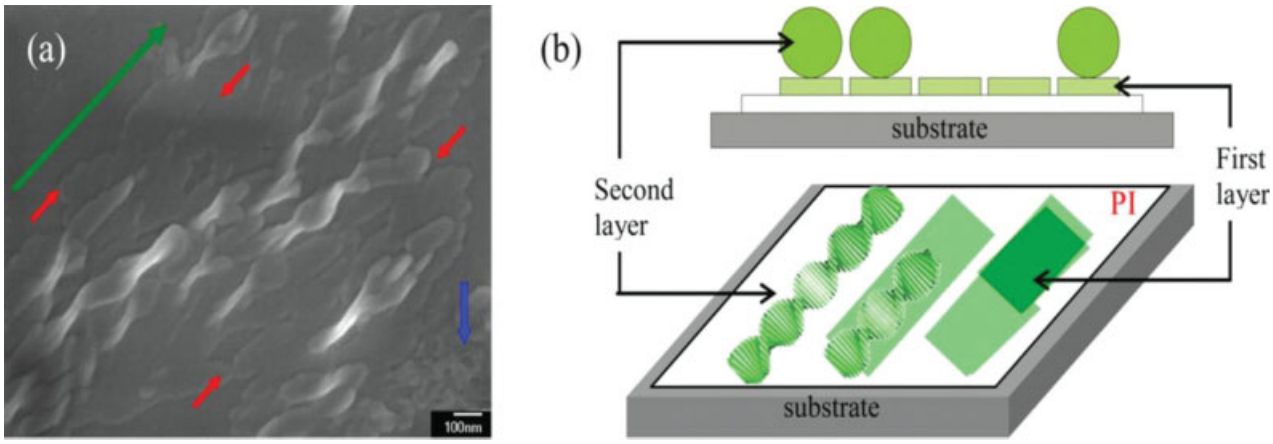

Figure 8. FESEM observation of molecular ordering of helical **LC-11** on rubbed PI substrate. (a) FESEM image of the epitaxial **LC-11**. The green arrow indicates the rubbing direction. The red arrows indicate the direction of epitaxial growth molecules. The blue arrow indicates the formless aggregations. The 2D self-assembled **LC-11** with right-handed helices can be clearly seen. (b) Schematic illustration of the hierarchical superstructure of the self-assembled **LC-11** on a rubbed PI substrate. [Color figure can be viewed in the online issue, which is available at www.interscience.wiley.com.]

smectic arrangement on the rubbed PI substrate can be clearly resolved into individual right-handed helix packed parallel to each other. The elongate helices can be seen over lengths larger than 2 μm [Fig. 9(a)]. The oriented helical morphology also exhibited a highly birefringent

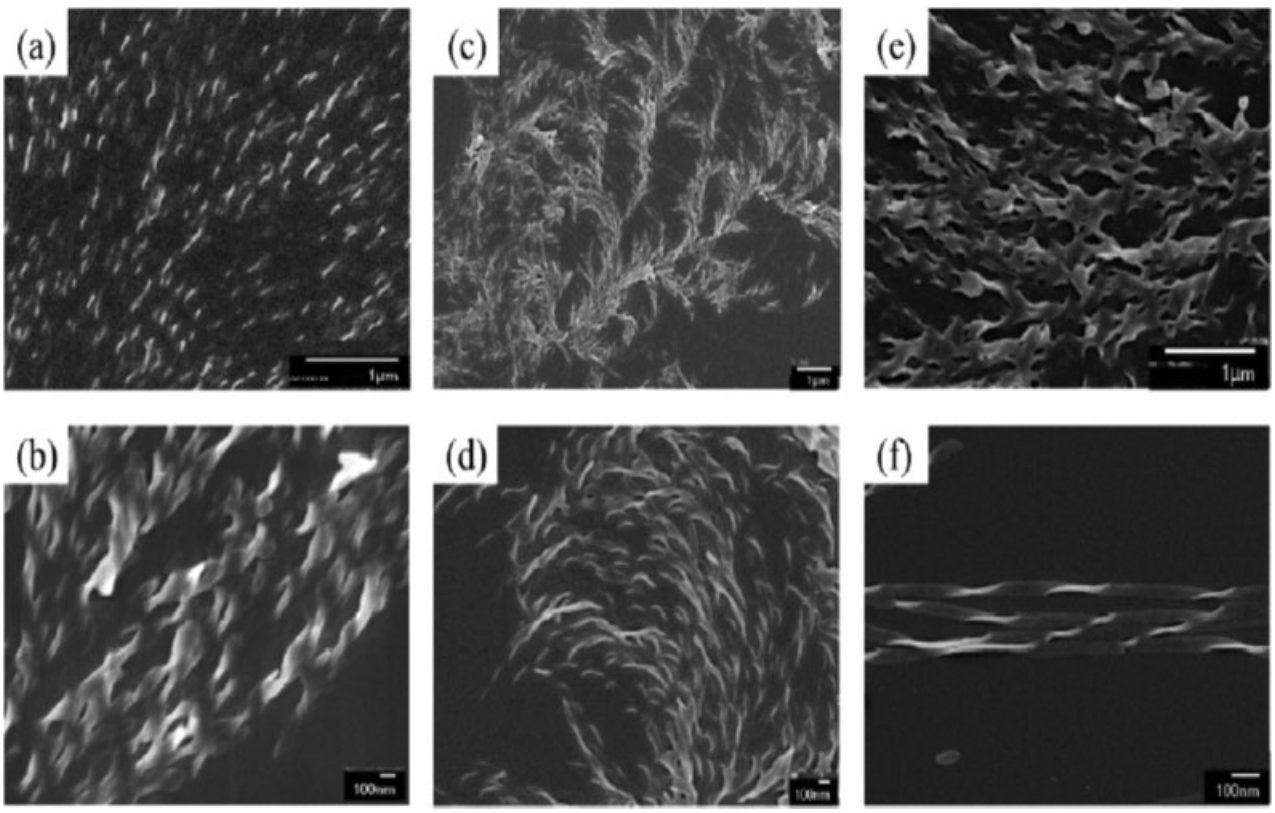

Figure 9. FESEM images of self-assembled helical structures of **LC-11** and their respective zoomed in images on each of following substrates: (a,b) rubbed PI substrate; (c,d) nonrubbed PI substrate; (e,f) HOPG substrate.

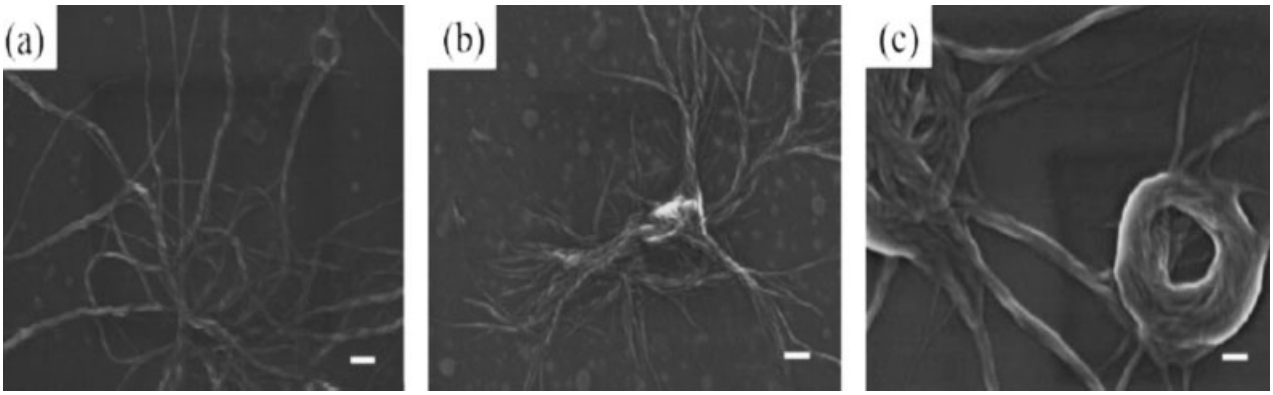

Figure 10. FESEM micrographs of the self-assembled morphologies exhibited by **LCP-11** in solution (a) primary stage, (b) intermediate stage, and (c) final stage. The bar represents 100 nm.

texture with a characteristic banded pattern perpendicular to the rubbing direction [Fig. 9(b)]. Therefore, the first layer of the **LC-11** epitaxially deposited on the basal plate of the rubbed PI substrate could not only prevent unfavorable direct interactions between molecules and surface but also serve as a template[38] for subsequent formation of the upper-layer helix with controlled helicity and packing.

To confirm the effect of the rubbing process on the orientation control to the PI surface, we used nonrubbed PI substrate as a comparison. The corresponding images from FESEM are shown in Figure 9. A nanostructure of helical morphology similar to that obtained from the rubbed PI substrate is observed [Fig. 9(d)]. However, in terms of the perfection of the ordering, the nanostructure produced on the nonrubbed PI substrate is much more defective with many more arced dislocations than when the rubbed substrate is used [Fig. 9(c)]. It was reported that rubbing treatment enhanced the degree of regularity and crystallinity of polymer chains at the surface region,[39] though studied PI is an amorphous polymer. We consider that the rubbing process is an effective way to induce molecular orientation onto a polymer layer. We also studied that **LC-11** self-assemble into 2D layered alignment on HOPG with ordered planar carbon lattices [Fig. 9(e,f)]. The observations for the morphology and degree of orientation on HOPG are not as well as on rubbed PI substrate. This result can be explained by considering the substrate surface energy (γ). According to the literature results,[40] the surface energy of PI substrate ($\gamma_{PI} = 0.038$ J m^{-2}) is much smaller than that of HOPG substrate ($\gamma_{HOPG} = 0.2$ J m^{-2}). In general, LC molecules prefer to stay on the low surface energy surface. The van der Waals dispersion interaction between LC molecules and the rubbed PI substrate is much stronger than that of LC molecules and HOPG substrate. Consequently, the rubbed PI film is found to be more effective to orient the epitaxial molecules in monolayer than HOPG.

Self-Assembled Hierarchical Superstructures of LC Polymers in Solution

The self-assembled hierarchical superstructure of LC polyacetylenes in solution was also investigated with FESEM. **LCP-11** aggregated to form helical nanofibers at primary stage [Fig. 10(a)] and some nanospheres at intermediate stage [Fig. 10(b)] when the nonsolvent, methanol, was added gradually into THF solution. This structural transition was due to the fact that THF tends to induce the polymer chains to twist into extended fibers, while methanol is inclined to promote the polymer chains to twine into micellar spheres. The balance of these two repulsive forces leads to the formation of the intermediate structures. In the final stage, the nanofibers are evolved from the helical cables ornamented with entwining nanofibers upon natural evaporation of the solution in a mixture of THF/methanol = 3/7 (v/v) [Fig. 10(c)]. Both the main chain helixes and chiral character of saccharide units are the driving forces for the polymer molecules to form complicated helical cables. **LCP-12** formed very similar helical morphology as **LCP-11** in methanol/THF solution while **LCP-6** did not form any helical morphology.

CONCLUSION

We have synthesized a series of chiral galactopyranoside-based 1,2,3-triazole liquid crystal

poly(alkylacetylenes) with different alkynyloxy chain lengths. Both LC monomers and polymers clearly show a chiral S_A mesomorphism. All the monomers exhibited liquid-crystalline-like behavior for self-assembly so as to create tunable self-assembled morphologies including platelets and helical twists. The self-organized polymers exhibit a mixed intermediate morphology, including nanospheres and helical nanofibers except for **LC-6**. This structural transformation seems to originate from the balance between the repulsive interactions of the interstrand association in a methanol solution and extended force in a THF solution of polymer chains. Subsequently, these fibers are coiled around to form the helical cables ornamented with entwining nanofibers. Considering the conventional self-assembling systems such as copolymers, homopolymers have been commonly believed to be difficult to self-assemble into well-defined morphological structures.[41] The results described here demonstrate that chiral homopolymers carrying saccharide pendants can assemble into well-defined supramolecular nanostructures. We also have demonstrated that helical **LC-11** could be highly aligned on the rubbed PI substrate. To the best of our knowledge, this may be the first example of the spontaneous formation of a large area orientation of helical morphology due to a rubbed induced alignment of molecules. In conclusion, the synthesized saccharide-containing LC monomers and polymers which will aggregate to form helical superstructures have potential applications in optical switching and sensors devices.

The authors thank the National Science Council and Ministry of Education (MOE ATU Program) for financial support.

REFERENCES AND NOTES

1. Hsu, C.-S. Prog Polym Sci 1997, 22, 829–871.
2. (a) McQuade, D. T.; Pullen, A. E.; Swager, T. M. Chem Rev 2000, 100, 2537–2574; (b) Zheng, J.; Swager, T. M. Adv Polym Sci 2005, 177, 151–179.
3. (a) Ho, P. K. H.; Kim, J.-S.; Burroughes, J. H.; Becker, H.; Li, S. F. Y.; Brown, T. M.; Cacialli, F.; Friend, R. H. Nature 2000, 404, 481–484; (b) Kulkarni, A. P.; Tonzola, C. J.; Babel, A.; Jenekhe, S. A. Chem Mater 2004, 16, 4556–4573; (c) Tabata, M.; Fukushima, T.; Sadahiro, Y. Macromolecules 2004, 37, 4342–4350; (d) Akcelrud, L. Prog Polym Sci 2003, 28, 875–962; (e) Inganäs, O.; Berggren, M.; Andersson, M. R.; Gustafsson, G.; Hjertberg, T.; Wennerström, O.; Dyreklev, P.; Granström, M. Synth Met 1995, 71, 2121–2124; (f) Burroughs, J. H.; Bradley, D. D. C.; Brown, A. R.; Marks, R. N.; Mackay, K.; Friends, R. H.; Burn, P. L.; Holms, A. B. Nature (London) 1990, 347, 539–541.
4. (a) Granström, M.; Petrisch, K.; Arias, A. C.; Lux, A.; Andersson, M. R.; Friend, R. H. Nature 1998, 395, 257–260; (b) Dennler, G.; Sariciftci, N. S. Proc IEEE 2005, 93, 1429–1439; (c) Coakley, K. M.; McGehee, M. D. Chem Mater 2004, 16, 4533–4542.
5. (a) Yang, S.-H.; Hsu, C.-S. J Polym Sci Part A: Polym Chem 2009, 47, 2713–2733; (b) Percec, V.; Rudick, J. G.; Peterca, M.; Heiney, P. A. J Am Chem Soc 2008, 130, 7503–7508; (c) Percec, V.; Rudick, J. G.; Peterca. M.; Aqad, E.; Imam, M. R.; Heiney, P. A. J Polym Sci Part A: Polym Chem 2007, 45, 4974–4987; (d) Rudick, J. G.; Percec, V. Acc Chem Res 2008, 41, 1641–1652; (e) Samorí, P.; Engelkamp, H.; de Witte, P. A. J.; Rowan, A. E.; Nolte, R. J. M.; Rabe, J. P. Adv Mater 2005, 17, 1265–1268; (f) Engelkamp, H.; Middelbeek, S.; Nolte, R. J. M. Science 1999, 284, 785–788; (g) Palmans, A. R. A.; Meijer, E. W. Angew Chem Int Ed 2007, 46, 8948–8968.
6. (a) Lam, J. W. Y.; Tang, B. Z. J Polym Sci Part A: Polym Chem 2003, 41, 2607–2629; (b) Lam, J. W. Y.; Dong, Y.; Luo, J.; Cheuk, K. K. L.; Xie, Z.; Tang, B. Z. Thin Solid Films 2002, 417, 143–146; (c) Dong, Y.; Lam, J. W. Y.; Peng, H.; Cheuk, K. K. L.; Kwok, H. S.; Tang, B. Z. Macromolecules 2004, 37, 6408–6417; (d) Ye, C.; Xu, G.; Yu, Z. Q.; Lam, J. W. Y.; Jang, J. H.; Peng, H. L.; Tu, Y. F.; Liu, Z. F.; Jeong, K. U.; Cheng, S. Z. D.; Chen, E. Q.; Tang, B. Z. J Am Chem Soc 2005, 127, 7668–7669; (e) Xing, C.; Lam, J. W. Y.; Zhao, K.; Tang, B. Z. J Polym Sci Part A: Polym Chem 2008, 46, 2960–2974; (f) Li, B. S.; Cheuk, K. K. L.; Salhi, F.; Lam, J. W. Y.; Cha, J. A. K.; Xiao, X.; Bai, C.; Tang, B. Z. Nano Lett 2001, 1, 323–328.
7. Pugh, C.; Percec, V. Mol Cryst Liq Cryst 1990, 178, 193–217.
8. (a) Oh, S. Y.; Akagi, K.; Shirakawa, H.; Araya, K. Macromolecules 1993, 26, 6203–6206; (b) Akagi, K.; Shirakawa, H. Macromol Symp 1996, 104, 137–158; (c) Goto, H.; Akagi, K.; Shirakawa, H. Synth Met 1997, 84, 373–374; (d) Goto, H.; Dai, X. M.; Ueoka, T.; Akagi, K. Macromolecules 2004, 37, 4783–4793.
9. (a) Ting, C.-H.; Hsu, C.-S. J Polym Res 2001, 8, 159–167; (b) Ting, C.-H.; Chen, J.-T.; Hsu, C.-S. Macromolecules 2002, 35, 1180–1189.
10. (a) Okoshi, K.; Sakajiri, K.; Kumaki, J.; Yashima, E. Macromolecules 2005, 38, 4061–4064; (b) Nagai, K.; Sakajiri, K.; Maeda, K.; Okoshi, K.; Sato, T.; Yashima, E. Macromolecules 2006, 39, 5371–5380.

11. Kang, S. W.; Jin, S. H.; Chien, L. C.; Sprunt, S. Adv Funct Mater 2004, 14, 329–334.
12. Chen, L.; Chen, Y.; Zha, D.; Yang, Y. J Polym Sci Part A: Polym Chem 2006, 44, 2499–2509.
13. Kwak, G.; Minakuchi, M.; Sakaguchi, T.; Masuda, T.; Fujiki, M. Chem Mater 2007, 19, 3654–3661.
14. Zhou, D.; Chen, Y.; Chen, L.; Zhou, W.; He, X. Macromolecules 2009, 42, 1454–1461.
15. (a) Yashima, E.; Maeda, K.; Okamoto, Y. Nature 1999, 399, 449–451; (b) Nakano, T.; Okamoto, Y. Chem Rev 2001, 101, 4013–4038; (c) Yamamoto, C.; Yashima, E.; Okamoto, Y. J Am Chem Soc 2002, 124, 12583–12589; (d) Hoshikawa, N.; Hotta, Y.; Okamoto, Y. J Am Chem Soc 2003, 125, 12380–12381; (e) Maeda, K.; Morino, K.; Okamoto, Y.; Sato, T.; Yashima, E. J Am Chem Soc 2004, 126, 4329–4342; (f) Yashima, E.; Maeda, K.; Nishimura, T. Chem Eur J 2004, 10, 42–51.
16. (a) Green, M. M.; Park, J.-W.; Sato, T.; Teramoto, A.; Lifson, S.; Selinger, R. L. B.; Selinger, J. V. Angew Chem Int Ed 1999, 38, 3138–3154; (b) Green, M. M.; Cheon, K.-S.; Yang, S.-Y.; Park, J.-W.; Swansburg, S.; Liu, W. Acc Chem Res 2001, 34, 672–680; (c) Tang, K.; Green, M. M.; Cheon, K.-S.; Selinger, J. V.; Garetz, B. A. J Am Chem Soc 2003, 125, 7313–7323.
17. (a) Cornelissen, J. J. L. M.; Rowan, A. E.; Nolte, R. J. M.; Sommerdijk, N. A. J. M. Chem Rev 2001, 101, 4039–4070; (b) Hill, D. J.; Mio, M. J.; Prince, R. B.; Hughes, T. S.; Moore, J. S. Chem Rev 2001, 101, 3893–4012.
18. (a) Aoki, T. Prog Polym Sci 1999, 24, 951–993; (b) Feringa, B. L.; van Delden, R. A.; Koumura, N.; Geertsema, E. M. Chem Rev 2000, 100, 1789–1816; (c) Pu, L. Macromol Rapid Commun 2000, 21, 795–809; (d) Fujiki, M. Macromol Rapid Commun 2001, 22, 539–563; (e) Aoki, T.; Kaneko, T. Polym J 2005, 37, 717–735.
19. Moore, J. S.; Gorman, C. B.; Grubbs, R. H. J Am Chem Soc 1991, 113, 1704–1712.
20. (a) Yashima, E.; Huang, S.; Matsushima, T.; Okamoto, Y. Macromolecules 1995, 28, 4184–4193; (b) Yashima, E.; Matsushima, T.; Okamoto, Y. J Am Chem Soc 1995, 117, 11596–11587; (c) Yashima, E.; Matsushima, T.; Okamoto, Y. J Am Chem Soc 1997, 119, 6345–6359; (d) Nakako, H.; Mayahara, Y.; Nomura, R.; Tabata, M.; Masuda, T. Macromolecules 2000, 33, 3978–3982.
21. (a) Li, B. S.; Cheuk, K. K. L.; Ling, L. S.; Chen, J. W.; Xiao, X. D.; Bai, C. L.; Tang, B. Z. Macromolecules 2003, 36, 77–85; (b) Gao, G.; Sanda, F.; Masuda, T. Macromolecules 2003, 36, 3932–3937; (c) Morino, K.; Oobo, M.; Yashima, E. Macromolecules 2005, 38, 3461–3468; (d) Sanda, F.; Terada, K.; Masuda, T. Macromolecules 2005, 38, 8149–8154; (e) Onouchi, H.; Hasegawa, T.; Kashiwagi, D.; Ishiguro, H.; Maeda, K.; Yashima, E. Macromolecules 2005, 38, 8625–8633; (f) Zhao, H.; Sanda, F.; Masuda, T. Polymer 2005, 46, 2841–2846.
22. (a) De Feyter, S.; De Schryver, F. C. Chem Soc Rev 2003, 32, 139–150; (b) Barlow, S. M.; Raval, R. Surf Sci Rep 2003, 50, 201–341.
23. (a) Giancarlo, L. C.; Flynn, G.W. Acc Chem Res 2000, 33, 491–501; (b) Ortega Lorenzo, M.; Baddeley, C. J.; Muryn, C.; Raval, R. Nature 2000, 404, 376–378; (c) Kühnle, A.; Linderoth, T. R.; Hammer, B.; Besenbacher, F. Nature 2002, 415, 891–893; (d) Fasel, R.; Parschau, M.; Ernst, K. H. Nature 2006, 439, 449–452.
24. (a) Sakurai, S.-I.; Okoshi, K.; Kumaki, J.; Yashima, E. Angew Chem Int Ed 2006, 45, 1245–1248; (b) Sakurai,S.-I.; Okoshi, K.; Kumaki, J.; Yashima, E. J Am Chem Soc 2006, 128, 5650–5651; (c) Onouchi, H.; Okoshi, K.; Kajitani, T.; Sakurai, S.-I.; Nagai, K.; Kumaki, J.; Onitsuka, K.; Yashima, E. J Am Chem Soc 2008, 130, 229–236.
25. Pfaendler, H. R.; Weimar, V. Synthesis 1996, 11, 1345–1349.
26. Fazio, F.; Bryan, M. C.; Blixt, O.; Paulson, J. C.; Wong, C.-H. J Am Chem Soc 2002, 124, 14397–14402.
27. (a) Cheuk, K. K. L.; Li, B. S.; Tang, B. Z. In Encyclopedia of Nanoscience and Nanotechnology; Nalwa, H. S., Ed.; American Scientific Publishers: Stevenson Ranch, CA, 2004; Vol. 8, pp 703–713; (b) Cheuk, K. K. L.; Lam, J. W. Y.; Sun, Q.; Cha, J. A. K.; Tang, B. Z. Polym Prepr 1999, 40, 655–656; (c) Yashima, E.; Maeda, K.; Sata, O. J Am Chem Soc 2001, 123, 8159–8160; (d) Li, B. S.; Cheuk, K. K. L.; Zhou, J.; Xie, Y.; Cha, J. A. K.; Xiao, X.; Tang, B. Z. Polym Prepr 2001, 42, 543–544; (e) Lai, L. M.; Lam, J. W. Y.; Qin, A.; Dong, Y.; Tang, B. Z. J Phys Chem B 2006, 110, 11128–11138.
28. (a) Tang, B. Z.; Kong, X.; Wan, X.; Feng, X. D. Macromolecules 1997, 30, 5620–5628; (b) Dai, X. M.; Gato, H.; Akagi, K.; Shirakawa, H. Synth Met 1999, 102, 1289–1290; (c) Lam, W. Y.; Kong, X.; Dong, Y.; Cheuk, K. L.; Xu, K.; Tang, B. Z. Macromolecules 2000, 33, 5027–5040; (d) Cheuk, K. K. L.; Lam, J. W. Y.; Chen, J.; Lai, L. M.; Tang, B. Z. Macromolecules 2003, 36, 5947–5959; (e) Cheuk, K. K. L.; Lam, J. W. Y.; Chen, J.; Lai, L. M.; Tang, B. Z. J Am Chem Soc 2000, 122, 8830–8836; (f) Sedláček, J.; Vohlídal, J. Collect Czech Chem Commun 2003, 68, 1745–1790.
29. Kong, X.; Lam, W. Y.; Tang, B. Z. Macromolecules 1999, 32, 1722–1730.
30. Tang, B. Z.; Kong, X.; Wan, X.; Peng, H.; Lam, W. Y.; Feng, X. D.; Kwok, H. S. Macromolecules 1998, 31, 2419–2432.
31. (a) Lam, J. W. Y.; Tang, B. Z. Acc Chem Res 2005, 38, 745–754; (b) Yuan, W. Z.; Qin, A.; Lam, J. W. Y.; Sun, J. Z.; Dong, Y.; Haussler, M.; Liu, J.; Xu, H. P.; Zheng, Q.; Tang, B. Z. Macromolecules 2007, 40, 3159–3166.

32. (a) Simionescu, C.; Dumitrescu, S.; Percec, V. J Polym Sci Polym Symp 1978, 64, 209–227; (b) Furlani, A.; Napoletano, C.; Russo, M. V.; Feast, W. J. Polym Bull 1986, 16, 311–317; (c) Furlani, A.; Licoccia, S.; Russo, M. V. J Polym Sci Part A: Polym Chem 1986, 24, 991–1005; (d) Furlani, A.; Napoletano, C.; Russo, M. V.; Marsich, N. J Polym Sci Part A: Polym Chem 1989, 27, 75–86; (e) Lee, D.-H.; Soga, K. Makromol Chem Rapid Commun 1990, 11, 559–563.
33. (a) Simionescu, C.; Dumitrescu, S.; Percec, V. Polym J 1976, 8, 139–149; (b) Simionescu, C.; Dumitrescu, S.; Percec, V. Polym J 1976, 8, 313–317; (c) Dumitrescu, S.; Percec, V.; Simionescu, C. I. J Polym Sci Part A: Polym Chem 1977, 15, 2893–2907; (d) Simionescu, C. I.; Percec, V.; Dumitrescu, S. J Polym Sci Part A: Polym Chem 1977, 15, 2497–2509.
34. (a) Sung, C.-H.; Kung, L.-R.; Hsu, C.-S.; Lin, T.-F.; Ho, R.-M. Chem Mater 2006, 18, 352–359; (b) Lin, T.-F.; Ho, R.-M.; Sung, C.-H.; Hsu, C.-S. Chem Mater 2006, 18, 5510–5519; (c) Lin, T.-F.; Ho, R.-M.; Sung, C.-H.; Hsu, C.-S. Chem Mater 2008, 24, 1404–1409.
35. (a) Handbook of Spectroscopy; Robinson, J. W., Ed.; CRC Press: Boca Raton, FL, 1981; (b) Silverstein, R. M.; Bassler, G. C.; Morrill, T. C. Spectrometric Identification of Organic Compounds, 5th ed.; Wiley: New York, 1991.
36. Tang, B. Z.; Kong, X.; Wan, X.; Peng, H.; Lam, W. Y.; Feng, X.-D.; Kwok, H. S. Macromolecules 1998, 31, 2419–2432.
37. Circular Dichroism: Principles and Applications; Nakanishi, K.; Berova, N.; Woody, R. W., Eds.; Wiley-VCH: New York, 2000.
38. Severin, N.; Barner, J.; Kalachev, A. A.; Rabe, J. P. Nano Lett 2004, 4, 577–579.
39. (a) Iinuma, Y.; Kishimoto, K.; Sagara, Y.; Yoshio, M.; Mukai, T.; Kobayashi, I.; Ohno, H.; Kato, T. Macromolecules 2007, 40, 4874–4878; (b) Toney, M. F.; Russell, T. P.; Logan, J. A.; Kikuchi, H.; Sands, J. M.; Kumar, S. K. Nature (London) 1995, 374, 709–711; (c) Geary, J. M.; Goodby, J. W.; Kmetz, A. R.; Patel, J. S. J Appl Phys 1987, 62, 4100–4108.
40. (a) Chen, Y.; Iroh, J. O. Chem Mater 1999, 11, 1218–1222; (b) Gimeno, Y.; Hernández-Creus, A.; González, S.; Azzaroni, O.; Schilardi, P. L.; Salvarezza, R. C. Nanotechnology 2004, 15, 82–85.
41. Yu, S. M.; Soto, C. M.; Tirrell, D. A. J Am Chem Soc 2000, 122, 6552–6559.